Experimental study on the sound absorption characteristics of continuously graded phononic crystals

Cite as: AIP Advances **6**, 105205 (2016); https://doi.org/10.1063/1.4965923
Submitted: 19 April 2016 • Accepted: 08 October 2016 • Published Online: 17 October 2016

X. H. Zhang, Z. G. Qu, X. C. He, et al.

Experimental study on the sound absorption characteristics of continuously graded phononic crystals

X. H. Zhang, Z. G. Qu,[a] X. C. He, and D. L. Lu
Key Laboratory of Thermo-Fluid Science and Engineering of Ministry of Education, School of Energy and Power Engineering, Xi'an Jiaotong University, Xi'an 710049, P.R. China

(Received 19 April 2016; accepted 8 October 2016; published online 17 October 2016)

Novel three-dimensional (3D) continuously graded phononic crystals (CGPCs) have been designed, and fabricated by 3D printing. Each of the CGPCs is an entity instead of a combination of several other samples, and the porosity distribution of the CGPC along the incident direction is nearly linear. The sound absorption characteristics of CGPCs were experimentally investigated and compared with those of uniform phononic crystals (UPCs) and discretely stepped phononic crystals (DSPCs). Experimental results show that CGPCs demonstrate excellent sound absorption performance because of their continuously graded structures. CGPCs have higher sound absorption coefficients in the large frequency range and more sound absorption coefficient peaks in a specific frequency range than UPCs and DSPCs. In particular, the sound absorption coefficients of the CGPC with a porosity of 0.6 and thickness of 30 mm are higher than 0.56 when the frequency is 1350–6300 Hz and are all higher than 0.2 in the studied frequency range (1000–6300 Hz). CGPCs are expected to have potential application in noise control, especially in the broad frequency and low-frequency ranges. [http://dx.doi.org/10.1063/1.4965923]

I. INTRODUCTION

Phononic crystals (PCs) consist of periodic structures that are engineered to manipulate acoustic wave propagation.[1,2] Since PCs were first proposed by Kushwaha et al.,[2] much attention has been devoted to PCs because of their substantial applications in waveguide,[3] sound attenuation,[4] absorber,[5,6] sound insulation,[7] acoustic lens,[8] enhanced inertia,[9] shield,[10] filtering,[11,12] sensor,[13] strong reflectors for surface acoustic waves,[14–16] and microfluidic manipulations.[17,18] In addition, PCs give rise to novel effects, such as negative refraction,[19–21] negative birefraction,[22] negative elastic modulus,[23] and negative mass density.[24,25]

Continuously graded phononic crystals (CGPCs) and discretely stepped phononic crystals (DSPCs) are special types of PCs with continuously graded or discretely stepped structures. CGPCs possess designed continuous change in their structures and properties, whereas DSPCs possess stepwise change.[26–28] Research on gradient/graded PCs includes gradient-index acoustic lens,[27,29–31] acoustic focusing,[32,33] and acoustic mirage.[34] Several studies have been devoted to the sound absorption characteristics of PCs, and have indicated that PCs could be employed to expand the content of sound absorption materials.[35–38] To the best knowledge of the authors, no research has been conducted on the sound absorption characteristics of CGPCs.

In this paper, three-dimensional (3D) CGPCs are designed to experimentally investigate the sound absorption characteristics of CGPCs. The designed CGPCs, classified as solid–fluid (mixed) PCs,[39]

[a]Author to whom correspondence should be addressed. Electronic mail: zgqu@mail.xjtu.edu.cn.

are 3D lattice of air spheres immersed in a photosensitive resin background. The sound absorption performance of CGPCs is compared with that of DSPCs and uniform phononic crystals (UPCs), and CGPCs can be potentially applied in noise control.

II. MATERIALS AND METHODS

The 3D CGPCs are fabricated with photosensitive resin by means of 3D printing [Fig. 1(a)]. In previous studies,[3,11,19,22,38] the inclusions of PCs are solid and the backgrounds are fluid. By contrast, the backgrounds of the present CGPCs are solid and the inclusions are fluid, and these CGPCs are porous cylinders with continuously graded structures. Hence, the airborne inclusions are regarded as unit cells. The CGPCs possess another two characteristics: (1) each of the CGPCs is an entity instead of a combination of several other samples like DSPCs; (2) the porosity distribution of the CGPC along the incident direction is nearly linear. Fig. 1(b) shows the local structures of the CGPCs. The gradient of PCs is defined as the absolute value of the ratio of the change in porosity over the change in dimensionless thickness along the incident direction. And the dimensionless thickness is the ratio of the depth in the propagation direction over the total sample thickness. The porosity of the CGPC is altered by changing the pore diameter. Fig. 1(c) shows the variation in porosity and pore diameter along the incident direction of a CGPC, indicating that the lattice constants of CGPCs are within the homogenization limit (propagation wavelength $\lambda \geq 4a$, where a is the lattice constant).[29,33] UPCs are designed for reference. They are porous cylinders with uniform, periodic structures and produced using 3D printing [Fig. 2(a)]. The local structures and the variation in porosity and pore diameter along the incident direction of the UPC are constant, as illustrated in Figs. 2(b) and 2(c), respectively. Tables I and II show the geometric parameters, total porosity, and gradient of the CGPCs and UPCs, respectively, where the total porosity is defined as the total volume average of porosity over the entire sample thickness. For simplicity, CGPC-0.5-20 mm represents the CGPC sample with a total porosity of 0.5 and 20 mm in thickness. DSPCs, which are also designed for reference, comprise three UPC layers [Fig. 3(a)]. The schematic of the assembly of the DSPC is shown in Fig. 3(b), and the sequences

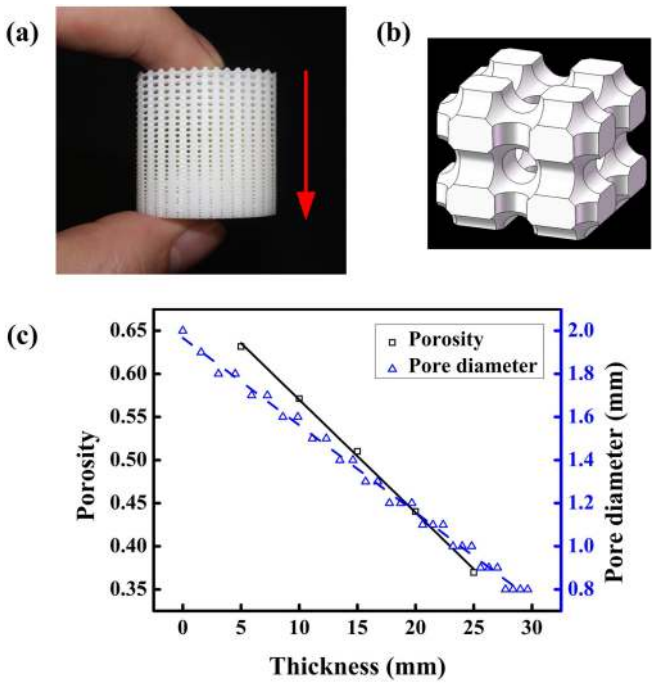

FIG. 1. CGPC with a sample diameter of 29.8 mm and a thickness of 30 mm. (a) Digital image, (b) local structures, and (c) variation in porosity and pore diameter along the incident direction. The red arrow is along the incident direction.

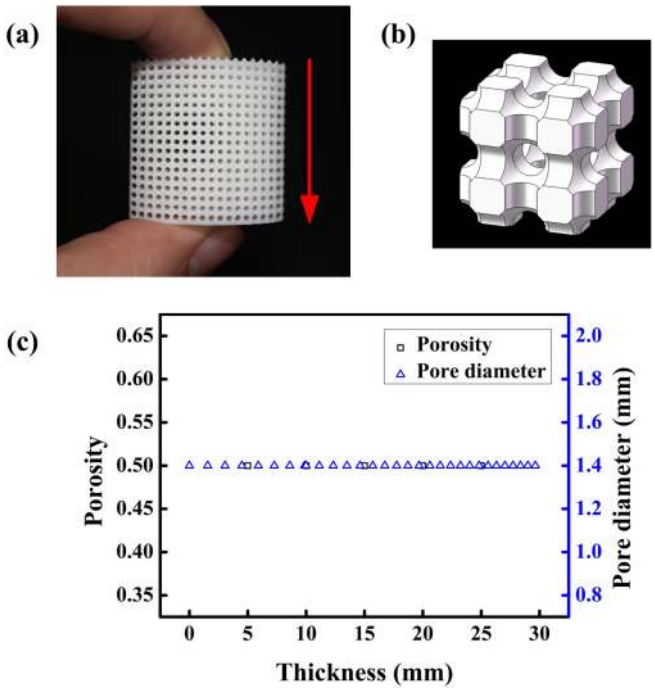

FIG. 2. UPC with a sample diameter of 29.8 mm and a thickness of 30 mm. (a) Digital image, (b) local structures, and (c) variation in porosity and pore diameter along the incident direction. The red arrow is along the incident direction.

of the assembly of DSPCs are presented in Table III. The UPCs for the assembly of DSPCs are presented in Table IV. According to $\lambda \geq 4a$ and $c = f\lambda$, one structure is in the homogenization limit if $c \geq 4af$. The DSPC-0.5-30 mm is taken for example. The sample DSPC-0.5-30 mm comprises UPC-0.4-10 mm, UPC-0.5-10 mm, and UPC-0.6-10 mm. The UPC-0.6-10 mm has the largest unit cell among the three UPCs. If the UPC-0.6-10 mm is in the homogenization limit with consideration of the largest measured frequency 6300 Hz, the sample DSPC-0.5-30 mm can be considered in the homogenization limit. The unit cell of the UPC-0.6-10 mm is arranged in a cube lattice with the length of 1.8 mm, the width of 1.8 mm, and the height of 1.6 mm. So, the largest lattice constant a is considered 1.8 mm. Hence, the sound speed for homogenization limit is $c \geq 45.36$ m/s which is one order smaller than sound speed 343 m/s for air. Therefore, the DSPC-0.5-30 mm is in the homogenization limit.

A material with a sound absorption coefficient that is larger than 0.2 is considered a sound absorption material, and a material with a sound absorption coefficient that is larger than 0.56 is considered an efficient sound absorption material.[40,41] In this experiment, the SW Type-477 impedance tube (BSWA Technology Co. Ltd, Beijing), using the standard procedure detailed in

TABLE I. Geometric parameters, total porosity, and gradient of CGPCs.

Sample No.	Description	Total porosity	Sample diameter (mm)	Thickness (mm)	Gradient[a]
CGPC-1	CGPC-0.4-20 mm	0.4	29.8	20	0.34
CGPC-2	CGPC-0.4-30 mm	0.4	29.8	30	0.38
CGPC-3	CGPC-0.5-20 mm	0.5	29.8	20	0.35
CGPC-4	CGPC-0.5-30 mm	0.5	29.8	30	0.39
CGPC-5	CGPC-0.6-20 mm	0.6	29.8	20	0.16
CGPC-6	CGPC-0.6-30 mm	0.6	29.8	30	0.17

[a]In this paper, the gradient is the absolute value of the ratio of the change in porosity over the change in dimensionless thickness along the incident direction.

TABLE II. Geometric parameters, total porosity, and gradient of UPCs.

Sample No.	Description	Total porosity	Sample diameter (mm)	Thickness (mm)	Gradient
UPC-1	UPC-0.4-20 mm	0.4	29.8	20	0
UPC-2	UPC-0.4-30 mm	0.4	29.8	30	0
UPC-3	UPC-0.5-20 mm	0.5	29.8	20	0
UPC-4	UPC-0.5-30 mm	0.5	29.8	30	0
UPC-5	UPC-0.6-20 mm	0.6	29.8	20	0
UPC-6	UPC-0.6-30 mm	0.6	29.8	30	0

ISO 10534-2:1998,[42] is applied to measure the sound absorption coefficients of PCs. The external diameter of the measured PC is 29.8 mm with consideration of tolerance, whereas the internal diameter of the SW Type-477 impedance tube is 30 mm. The measured frequency range is 1000 –6300 Hz. The side with large pores along the incident direction should be oriented to the sound source of the SW Type-477 impedance tube during the measurement of sound absorption coefficients of CGPCs.

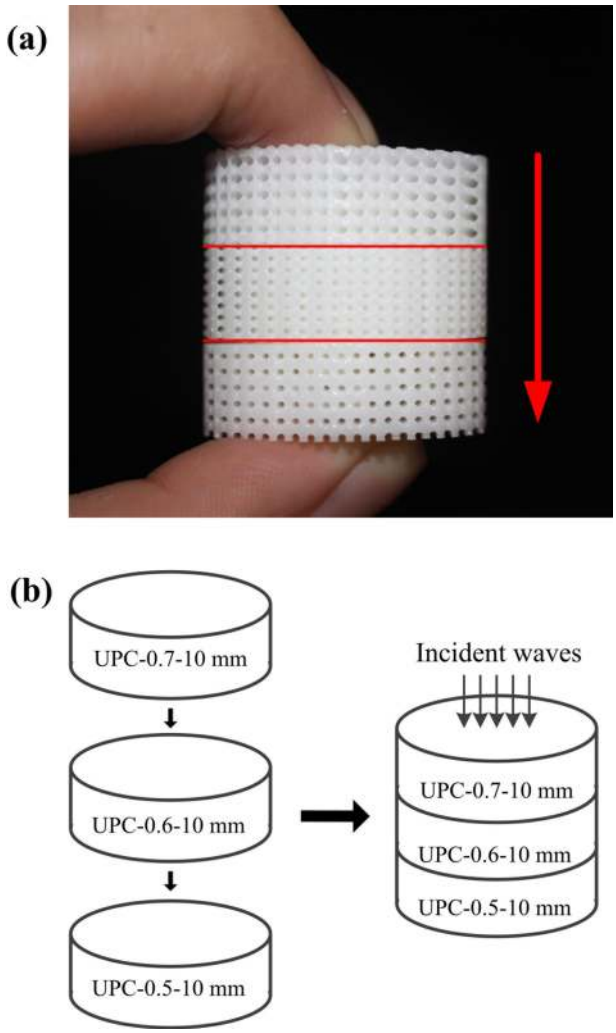

FIG. 3. DSPC comprising UPC-0.5-10 mm, UPC-0.6-10 mm, and UPC-0.7-10 mm. (a) Digital image; red lines are applied to distinguish the boundaries, and (b) schematic of the DSPC assembly. The red arrow is along the incident direction.

TABLE III. Assembling sequences of DSPCs.

Sample No.	Description	First layer	Second layer	Third layer
DSPC-1	DSPC-0.4-20 mm	UPC-S1	UPC-S3	UPC-S5
DSPC-2	DSPC-0.4-30 mm	UPC-S2	UPC-S4	UPC-S6
DSPC-3	DSPC-0.5-20 mm	UPC-S3	UPC-S5	UPC-S7
DSPC-4	DSPC-0.5-30 mm	UPC-S4	UPC-S6	UPC-S8
DSPC-5	DSPC-0.6-20 mm	UPC-S5	UPC-S7	UPC-S9
DSPC-6	DSPC-0.6-30 mm	UPC-S6	UPC-S8	UPC-S10

Note that the third layer is the closest to sound source.

TABLE IV. Geometric parameters, porosity, and gradient of UPCs for the assembly of DSPCs.

Sample No.	Description	Porosity	Sample diameter (mm)	Thickness (mm)	Gradient
UPC-S1	UPC-0.3-6.7 mm	0.3	29.8	6.7	0
UPC-S2	UPC-0.3-10 mm	0.3	29.8	10	0
UPC-S3	UPC-0.4-6.7 mm	0.4	29.8	6.7	0
UPC-S4	UPC-0.4-10 mm	0.4	29.8	10	0
UPC-S5	UPC-0.5-6.7 mm	0.5	29.8	6.7	0
UPC-S6	UPC-0.5-10 mm	0.5	29.8	10	0
UPC-S7	UPC-0.6-6.7 mm	0.6	29.8	6.7	0
UPC-S8	UPC-0.6-10 mm	0.6	29.8	10	0
UPC-S9	UPC-0.7-6.7 mm	0.7	29.8	6.7	0
UPC-S10	UPC-0.7-10 mm	0.7	29.8	10	0

III. SOUND ABSORPTION PERFORMANCE AND DISCUSSION

Six sets of experiments are performed to investigate the sound absorption performance of CGPCs. The sound absorption coefficients of the UPC, DSPC, and CGPC are measured at different total porosities and thicknesses. The total porosity values are 0.4, 0.5, and 0.6. The thicknesses are 20 and 30 mm.

Fig. 4(a) shows the sound absorption coefficients of the UPC, DSPC, and CGPC with a total porosity of 0.4 and thickness of 20 mm. The sound absorption coefficients of the three structures are all less than 0.2 at a frequency of less than 1700 Hz. This result implies that the sound absorption performance at a low-frequency range can still be improved. The peak values of the sound absorption coefficients are 0.94 (at 2900 Hz), 0.98 (at 3700 Hz), and 0.96 (at 3300 Hz) for UPC-0.4-20 mm, DSPC-0.4-20 mm, and CGPC-0.4-20 mm, respectively. The frequency ranges corresponding to the sound absorption coefficients that are higher than 0.56 for UPC-0.4-20 mm, DSPC-0.4-20 mm, and CGPC-0.4-20 mm are 2350–3600, 2900–6300, and 2600–4150 plus 5800–6300 Hz, respectively.

When the total porosity increases from 0.4 to 0.5 and 0.6 at a fixed thickness of 20 mm, the results are comparable with those shown in Figs. 4(a), 4(b), and 4(c). The peak value of UPC decreases from 0.94 (at 2900 Hz) to 0.81 (at 3100 Hz) and then to 0.72 (at 3300 Hz). The peak value of DSPC decreases from 0.98 (at 3700 Hz) to 0.79 (at 3550 Hz) and then to 0.7 (at 4100 Hz). The sound absorption characteristics of CGPC are augmented significantly. In particular, the two peaks for CGPC-0.6-20 mm are 0.98 (at 2300 Hz) and 0.97 (at 5300 Hz). The turning point frequency, below which the absorption coefficient is less than 0.2, decreases to 1380 Hz for CGPC-0.6-20 mm. The frequency ranges, above which the sound absorption coefficients are above 0.56, are broadened (1800–3000 Hz plus 4400–6300 Hz).

When the thickness varies from 20 mm to 30 mm, as shown in Fig. 4(d), the sound absorption coefficient peaks of UPC-0.4-30 mm, DSPC-0.4-30 mm, and CGPC-0.4-30 mm all shift to lower frequency due to the increase of the flow resistance and the sound dissipation.[43] The sound absorption coefficients of DSPC-0.4-30 mm and CGPC-0.4-30 mm are higher than those of UPC-0.4-30 mm when frequency increases from 2200 Hz to 5600 Hz. The sound absorption performances

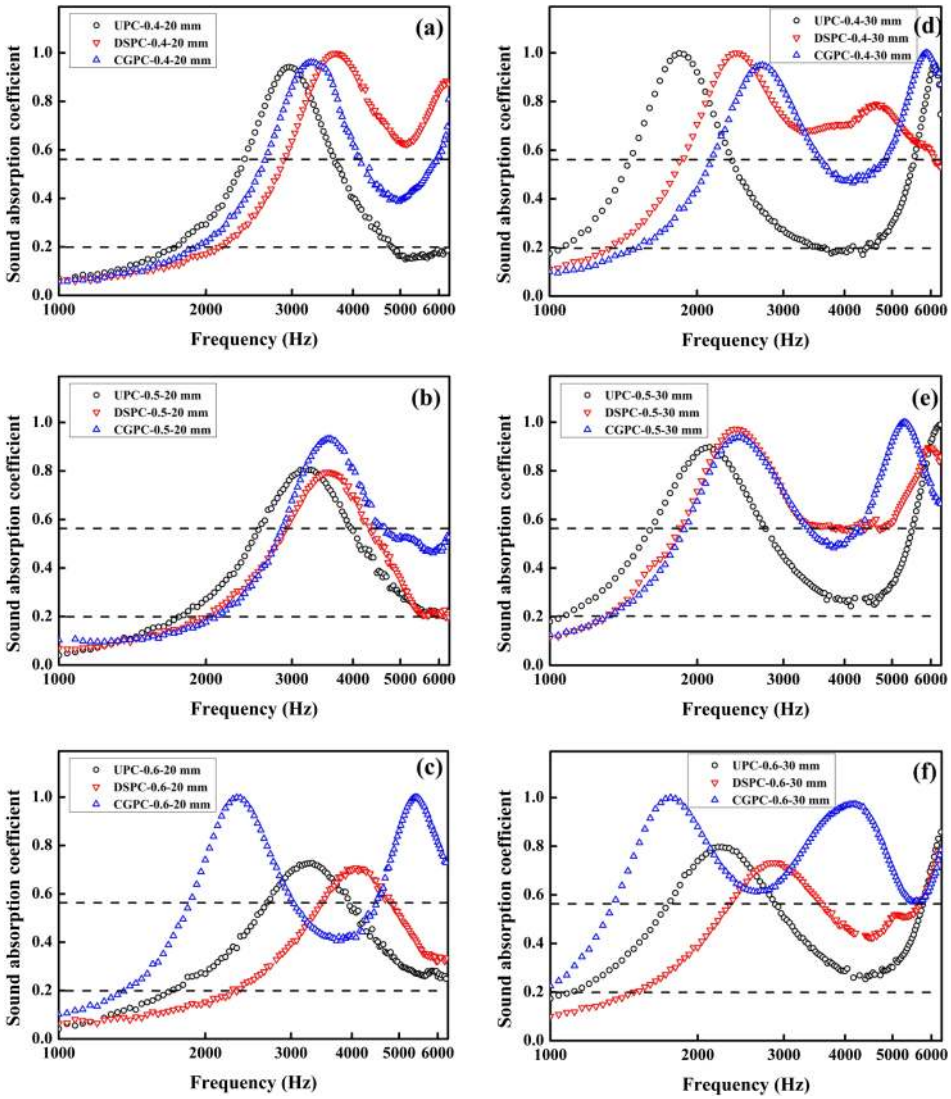

FIG. 4. Sound absorption coefficients of (a) UPC-0.4-20 mm, DSPC-0.4-20 mm, and CGPC-0.4-20 mm; (b) UPC-0.5-20 mm, DSPC-0.5-20 mm, and CGPC-0.5-20 mm; (c) UPC-0.6-20 mm, DSPC-0.6-20 mm, and CGPC-0.6-20 mm; (d) UPC-0.4-30 mm, DSPC-0.4-30 mm, and CGPC-0.4-30 mm; (e) UPC-0.5-30 mm, DSPC-0.5-30 mm, and CGPC-0.5-30 mm; and (f) UPC-0.6-30 mm, DSPC-0.6-30 mm, and CGPC-0.6-30 mm.

in the low-frequency range for UPC, DSPC, and CGPC all improve compared with that of their 20 mm-thick counterparts. In addition, the sound absorption performance in the high-frequency range greatly extended for CGPC and DSPC. The frequency ranges corresponding to an absorption coefficient that is higher than 0.56, are 1400–2300 Hz plus 5500–6300 Hz for UPC-0.4-30 mm, 1880–6000 Hz for DSPC-0.4-30 mm, and 2100–3600 Hz plus 4800–6300 Hz for CGPC-0.4-30 mm. The comparison results imply that an increase in thickness improves sound absorption performance. A similar improvement can be found in CGPC and DSPC with an increase in thickness at the total porosity of 0.5 and 0.6 compared with Figs. 4(b) and 4(e), and Figs. 4(c) and 4(f), respectively. In particular, CGPC-0.6-30 mm has the most superior sound absorption performance at a sound absorption coefficient of over 0.56 in a wide frequency range [Fig. 4(f)]. The values of the two sound absorption peaks are 0.99 and 0.97. The high sound absorption coefficients (higher than 0.56) are obtained when the frequency is higher than 1350 Hz and the sound absorption coefficients are all higher than 0.2 in the studied frequency range. Generally, CGPC-0.6-20 mm and CGPC-0.6-30 mm both have two peaks, whereas DSPC-0.6-20 mm, DSPC-0.6-30 mm, UPC-0.6-20 mm, and UPC-0.6-30 mm have

one peak within the measured frequency range (1000–6300 Hz). These results suggest that CGPCs display more sound absorption coefficient peaks at a specific frequency range than UPCs and DSPCs, and hence more significant broadband sound absorption performance.

The excellent sound absorption performance of CGPCs mentioned above may be attributed to the nearly linear porosity distribution along the incident direction caused by the continuously graded structures. Common sound absorption materials include porous sound absorption materials and resonant sound absorption materials.[44] In porous sound absorption materials, the incident acoustic energy is primarily converted into heat due to viscous and thermal losses at the walls of the interior pores and tunnels. It is a feasible measure to improve sound absorption coefficients by letting as much incident waves as possible propagate into sound absorption materials. The large pores close to the sound source make acoustic waves easy to propagate into CGPCs, and thus the materials have less reflection and more propagated acoustic energy. The Johnson-Champoux-Allard model (JCA model)[45,46] has been adopted to simulate the acoustic wave propagation and estimate the performance of traditional porous materials,[47,48] and five parameters (i.e. porosity, flow resistivity, tortuosity, characteristic viscous length and characteristic thermal length) are needed in the JCA model. However, the porosity in the JCA model is considered uniform, so all these five parameters can not reflect the porosity distribution of the CGPC when the porosity of the sample is not uniform. Development of the JCA model can be a challenge for future work.

The difference between the CGPC and the traditional resonant sound absorption material is caused by gradually changing the pore diameter in CGPCs as well. Helmholtz resonators might play a role in the demonstration of the sound absorption characteristics of the CGPCs. The CGPCs may have more resonators due to different pore diameters, which result in two sound absorption peaks of the CGPC with 20 mm in thickness, whereas the UPC and DSPC only have one peak when the sample thickness is 20 mm (Fig. 4).

The continuously graded configuration of the structures and the complicated acoustic propagation path of CGPCs assist in the dissipation of more energy, thus resulting in superior sound absorption performance. However, the mechanism of strong acoustic absorption in the CGPCs needs to be further investigated, because the size of the pore is variational along the incident direction.

IV. CONCLUSIONS

In summary, novel 3D CGPCs are designed and fabricated with photosensitive resin by means of 3D printing. The sound absorption performance of CGPCs is experimentally studied and compared with that of UPCs and DSPCs. Experimental results show that, compared with UPCs and DSPCs, CGPCs demonstrate more efficient sound absorption performance at a large frequency range, a better sound absorption performance at a low-frequency range, and possibly a greater number of sound absorption peaks at a specific frequency range. In particular, the sound absorption coefficients of CGPC-0.6-30 mm are higher than 0.56 at 1350-6300 Hz, and are all higher than 0.2 in the studied frequency range (1000–6300 Hz). CGPCs may have potential application in noise control, especially at broad and low-frequency ranges.

ACKNOWLEDGMENTS

This work was financially sponsored by the National Natural Science Foundation of China (No. 51322604) and National Program for Support of Top-notch Young Professionals.

[1] E. Yablonovitch, Physical review letters **58**(20), 2059–2062 (1987).
[2] M. S. Kushwaha, P. Halevi, L. Dobrzynski, and B. Djafari-Rouhani, Physical review letters **71**(13), 2022–2025 (1993).
[3] A. Khelif, A. Choujaa, S. Benchabane, B. Djafari-Rouhani, and V. Laude, Applied Physics Letters **84**(22), 4400 (2004).
[4] M. Hirsekorn, Applied Physics Letters **84**(17), 3364 (2004).
[5] M. D. Guild, V. M. García-Chocano, W. Kan, and J. Sánchez-Dehesa, Journal of Applied Physics **117**(11), 114902 (2015).
[6] T. Frenzel, J. David Brehm, T. Bückmann, R. Schittny, M. Kadic, and M. Wegener, Applied Physics Letters **103**(6), 061907 (2013).
[7] K. Lu, J. H. Wu, D. Guan, N. Gao, and L. Jing, AIP Advances **6**(2), 025116 (2016).
[8] S. Alagoz, O. A. Kaya, and B. B. Alagoz, Applied Acoustics **70**(11-12), 1400–1405 (2009).
[9] M. D. Guild, V. M. Garcia-Chocano, W. Kan, and J. Sánchez-Dehesa, AIP Advances **4**(12), 124302 (2014).
[10] K. M. Ho, C. K. Cheng, Z. Yang, X. X. Zhang, and P. Sheng, Applied Physics Letters **83**(26), 5566 (2003).

[11] R. Picó, V. J. Sánchez-Morcillo, I. Pérez-Arjona, and K. Staliunas, Applied Acoustics **73**(4), 302–306 (2012).
[12] Z. Zhao, Z. Qian, and B. Wang, AIP Advances **6**(1), 015002 (2016).
[13] M. Zubtsov, R. Lucklum, M. Ke, A. Oseev, R. Grundmann, B. Henning, and U. Hempel, Sensors and Actuators A: Physical **186**, 118–124 (2012).
[14] V. Laude, L. Robert, W. Daniau, A. Khelif, and S. Ballandras, Applied Physics Letters **89**(8), 083515 (2006).
[15] K. Kokkonen, M. Kaivola, S. Benchabane, A. Khelif, and V. Laude, Applied Physics Letters **91**(8), 083517 (2007).
[16] T.-T. Wu, W.-S. Wang, J.-H. Sun, J.-C. Hsu, and Y.-Y. Chen, Applied Physics Letters **94**(10), 101913 (2009).
[17] R. Wilson, J. Reboud, Y. Bourquin, S. L. Neale, Y. Zhang, and J. M. Cooper, Lab on a chip **11**(2), 323–328 (2011).
[18] Y. Bourquin, R. Wilson, Y. Zhang, J. Reboud, and J. M. Cooper, Advanced materials **23**(12), 1458–1462 (2011).
[19] E. Cubukcu, K. Aydin, E. Ozbay, S. Foteinopoulou, and C. M. Soukoulis, Nature **423**(6940), 604-605 (2003).
[20] S. Foteinopoulou and C. M. Soukoulis, Physical Review B **67**(23) (2003).
[21] X. Zhang and Z. Liu, Applied Physics Letters **85**(2), 341 (2004).
[22] M. H. Lu, C. Zhang, L. Feng, J. Zhao, Y. F. Chen, Y. W. Mao, J. Zi, Y. Y. Zhu, S. N. Zhu, and N. B. Ming, Nature materials **6**(10), 744–748 (2007).
[23] N. Fang, D. Xi, J. Xu, M. Ambati, W. Srituravanich, C. Sun, and X. Zhang, Nature materials **5**(6), 452–456 (2006).
[24] J. Mei, Z. Liu, W. Wen, and P. Sheng, Physical review letters **96**(2), 024301 (2006).
[25] Y. Ding, Z. Liu, C. Qiu, and J. Shi, Physical review letters **99**(9), 093904 (2007).
[26] E. Akmansoy, E. Centeno, K. Vynck, D. Cassagne, and J.-M. Lourtioz, Applied Physics Letters **92**(13), 133501 (2008).
[27] S.-C. S. Lin, T. J. Huang, J.-H. Sun, and T.-T. Wu, Physical Review B **79**(9) (2009).
[28] X. Miao and D. Sun, Materials **3**(1), 26–47 (2010).
[29] T. P. Martin, M. Nicholas, G. J. Orris, L.-W. Cai, D. Torrent, and J. Sánchez-Dehesa, Applied Physics Letters **97**(11), 113503 (2010).
[30] L. Zigoneanu, B.-I. Popa, and S. A. Cummer, Physical Review B **84**(2), 024305 (2011).
[31] T. P. Martin, C. J. Naify, E. A. Skerritt, C. N. Layman, M. Nicholas, D. C. Calvo, G. J. Orris, D. Torrent, and J. Sánchez-Dehesa, Physical Review Applied **4**(3), 034003 (2015).
[32] S. Peng, Z. He, H. Jia, A. Zhang, C. Qiu, M. Ke, and Z. Liu, Applied Physics Letters **96**(26), 263502 (2010).
[33] A. Climente, D. Torrent, and J. Sánchez-Dehesa, Applied Physics Letters **97**(10), 104103 (2010).
[34] S.-C. S. Lin and T. J. Huang, Journal of Applied Physics **106**(5), 053529 (2009).
[35] H. Zhao, Y. Liu, D. Yu, G. Wang, J. Wen, and X. Wen, Journal of Sound and Vibration **303**(1), 185–194 (2007).
[36] H. Zhao, Y. Liu, J. Wen, D. Yu, and X. Wen, Physics Letters A **367**(3), 224–232 (2007).
[37] H. Jiang, Y. Wang, M. Zhang, Y. Hu, D. Lan, Y. Zhang, and B. Wei, Applied Physics Letters **95**(10), 104101 (2009).
[38] C. J. Naify, T. P. Martin, C. N. Layman, M. Nicholas, A. L. Thangawng, D. C. Calvo, and G. J. Orris, Applied Physics Letters **104**(7), 073505 (2014).
[39] Y. Pennec, J. O. Vasseur, B. Djafari-Rouhani, L. Dobrzyński, and P. A. Deymier, Surface Science Reports **65**(8), 229–291 (2010).
[40] J. Lin, J. Guo, Y. Zhao, L. Duan, and S. Jin, Acta Materiae Compositae Sinica **31**(6), 1476–1480 (2014) (in Chinese).
[41] L. Wang, *Architectural decoration engineering materials* (Peking University Press, Beijing, 2006) (in Chinese).
[42] ISO 10534-2, (1998).
[43] F. Han, G. Seiffert, Y. Zhao, and B. Gibbs, Journal of Physics D: Applied Physics **36**(3), 294–302 (2003).
[44] X. Sagartzazu, L. Hervella-Nieto, and J. M. Pagalday, Archives of Computational Methods in Engineering **15**(3), 311–342 (2008).
[45] D. L. Johnson, J. Koplik, and R. Dashen, Journal of fluid mechanics **176**, 379–402 (1987).
[46] Y. Champoux and J. F. Allard, Journal of applied physics **70**(4), 1975–1979 (1991).
[47] X. H. Yang, S. W. Ren, W. B. Wang, X. Liu, F. X. Xin, and T. J. Lu, Composites Science and Technology **118**, 276–283 (2015).
[48] N. Kino, Applied Acoustics **96**, 153–170 (2015).